

Provided for non-commercial research and education use.  
Not for reproduction, distribution or commercial use.



This article appeared in a journal published by Elsevier. The attached copy is furnished to the author for internal non-commercial research and education use, including for instruction at the authors institution and sharing with colleagues.

Other uses, including reproduction and distribution, or selling or licensing copies, or posting to personal, institutional or third party websites are prohibited.

In most cases authors are permitted to post their version of the article (e.g. in Word or Tex form) to their personal website or institutional repository. Authors requiring further information regarding Elsevier's archiving and manuscript policies are encouraged to visit:

<http://www.elsevier.com/copyright>



Contents lists available at ScienceDirect

Physica C

journal homepage: [www.elsevier.com/locate/physc](http://www.elsevier.com/locate/physc)

## Effects of dilute columnar defects on the vortex matter in $\text{Bi}_2\text{Sr}_2\text{CaCu}_2\text{O}_{8+\delta}$ near the disorder-driven phase transition

D. Levi<sup>a,\*</sup>, A. Shaulov<sup>a</sup>, T. Tamegai<sup>b</sup>, Y. Yeshurun<sup>a</sup><sup>a</sup>Center for High- $T_c$  Superconductivity and Institute for Nanotechnology, Department of Physics, Bar-Ilan University, Ramat-Gan 52900, Israel<sup>b</sup>Department of Applied Physics, The University of Tokyo, Hongo, Bunkyo-ku, Tokyo 113-8656, Japan

## ARTICLE INFO

## Article history:

Received 8 February 2010

Accepted 25 April 2010

Available online 29 April 2010

## Keywords:

Vortex phase

Metastable disordered vortex state

Columnar defects

## ABSTRACT

Magneto-optical measurements are employed to characterize the disorder-driven vortex phase transition and the metastable disordered vortex state in heavy-ion irradiated and pristine regions of the same  $\text{Bi}_2\text{Sr}_2\text{CaCu}_2\text{O}_{8+\delta}$  crystal. We find that dilute columnar defects, while hardly affect the disorder-driven phase transition line, significantly increase the lifetime of the metastable state created in the vicinity of this line. Study of flux injection from the pristine region into the irradiated region suggests that in presence of columnar defects a metastable disordered state may be created in the bulk, in addition to being injected from the edges.

© 2010 Elsevier B.V. All rights reserved.

### 1. Introduction

Experimental and theoretical studies have revealed remarkable effects of columnar defects (CD) on the dynamic and thermodynamic properties of the vortex matter in high- $T_c$  superconductors [1–15]. Early investigations, focused on the limit of high density of CD, have shown that in this case the vortex matter forms a Bose glass phase that melts through a continuous transition [1,2]. Recent studies have concentrated on the opposite limit of dilute CD, where vortices outnumber CD at the relevant fields [3–15]. In this case the vortex matter can no longer be regarded as a homogenous pinned medium. Instead, two distinct subsystems of vortices are created: vortices pinned on the CD forming a rigid disordered array, and interstitial vortices which are relatively ordered at low temperatures and fields [5–7]. Investigations of the melting process have shown that the melting line of the interstitial vortices subsystem is shifted upwards with respect to the pristine melting line [5]. At the delocalization transition line, which is located further up, the rigid matrix of the vortices residing at the CD delocalizes and the vortex liquid becomes homogenous [5].

While the effect of dilute CD on the melting process is well established, their effect on the dynamic and thermodynamic properties of the vortex matter near the disorder-driven solid–solid transition is yet unclear. The present paper addresses this issue using magneto-optical measurements and analysis of the local magnetic response to external fields ramped at different rates. Presumably, upon increasing the field at low temperatures, only the

interstitial vortices undergo the solid–solid transition, while the vortices trapped in the randomly distributed CD remain unaffected. Thus, the separate melting and delocalization lines are supposed to merge at low temperatures into a single solid–solid transition line. Realizing that the melting and the solid–solid transition lines are two segments of the same order–disorder phase transition line [16,17], one may expect that dilute CD also shift the thermodynamic solid–solid transition line upwards. By contrast, our results indicate that dilute CD hardly affect the solid–solid transition line, tending to shift it slightly downward rather than upward.

The present paper also addresses the question of how CD affect the metastable disordered state (MDS) generated below the solid–solid transition line [18–29]. This metastable state is believed to be created by injection of vortices through inhomogeneous surface barriers while the external magnetic field increases [18–20]. As the induction of the transition is approached, the free energies of the quasi-ordered and the disordered states become comparable, and therefore the lifetime of the transient disordered phase becomes longer, diverging at the transition induction [19]. The effect of dilute CD on the MDS was investigated in  $\text{NbSe}_2$ , revealing enhancement of the MDS as compared to the pristine material, in contrast to the expectation that CD stretch the entangled vortices of the MDS and assist their annealing [11]. In the present work we characterize this effect quantitatively by measuring the lifetime,  $\tau(B, T)$ , of the MDS in the pristine and irradiated parts of the same  $\text{Bi}_2\text{Sr}_2\text{CaCu}_2\text{O}_{8+\delta}$  crystal. The existence of the MDS in our local magnetic measurements is manifested by a shift of the onset of the second magnetization peak to lower inductions as the sweep rate of the external field increases [22]. Utilizing this shift to determine

\* Corresponding author. Tel.: +972 3 5318607; fax: +972 3 7369599.  
E-mail address: [ph100@mail.biu.ac.il](mailto:ph100@mail.biu.ac.il) (D. Levi).

$\tau$  [28] reveals that the CD significantly increase the lifetime of the MDS, allowing the MDS to exist in the sample at low inductions, far below the transition, where in a pristine sample their lifetime is practically zero.

The configuration of our sample also allowed studying the generation of MDS as a result of injection of ordered vortices through an interface separating the pristine and the irradiated regions of the same sample. Our measurements show that such MDS are in fact created and that their lifetime matches that of the MDS injected through the natural sample edges. The injection of MDS within the bulk of the sample challenges the commonly accepted view that edge contaminations are the sole source responsible for the creation of MDS.

## 2. Experimental

Measurements were performed on a  $2.3 \times 1 \times 0.04 \text{ mm}^3$   $\text{Bi}_2\text{Sr}_2\text{CaCu}_2\text{O}_{8+\delta}$  single crystal ( $T_c = 92 \text{ K}$ ) grown by the floating zone method [30]. Part of the sample (right to the white dotted line in Fig. 1) was irradiated at the GSI Helmholtz Centre for Heavy Ion Research (Darmstadt, Germany), with 2.2 GeV Au ions (fluence of  $10^8 \text{ ions/cm}^2$ ) resulting in the formation of columnar defects of diameter 7–12 nm [31] with density corresponding to a matching field of 80 G. The range of the ion tracks was large enough to completely penetrate the 40  $\mu\text{m}$  thick crystal. The irradiation was performed at room temperature and under normal beam incidence. Local magnetization curves were extracted from magneto-optical images of the induction distribution, taken using an iron-garnet indicator with in-plane anisotropy and a 12 bit Hamamatsu CCD camera with a frame rate between 0.1 and 25 Hz. In a typical magneto-optical measurement, the sample was zero-field cooled to a target temperature between 24 and 32 K and was then subjected to external field parallel to the crystallographic  $c$ -axis of the sample. The external magnetic field was ramped up at a constant rate between 2.5 and 160 Oe/s, from 0 to about 700 Oe. Camera integration time used for image acquisition was 14–36 ms.

## 3. Results and discussion

Fig. 1 depicts magneto-optical images of the sample at  $T = 28 \text{ K}$  after exposing it to an external magnetic field ramped up from zero at a rate of 5 Oe/s. Flux penetration (brighter tone in the figure) is shown 7 s (a), 12 s (b) and 19 s (c) after the application of the field.

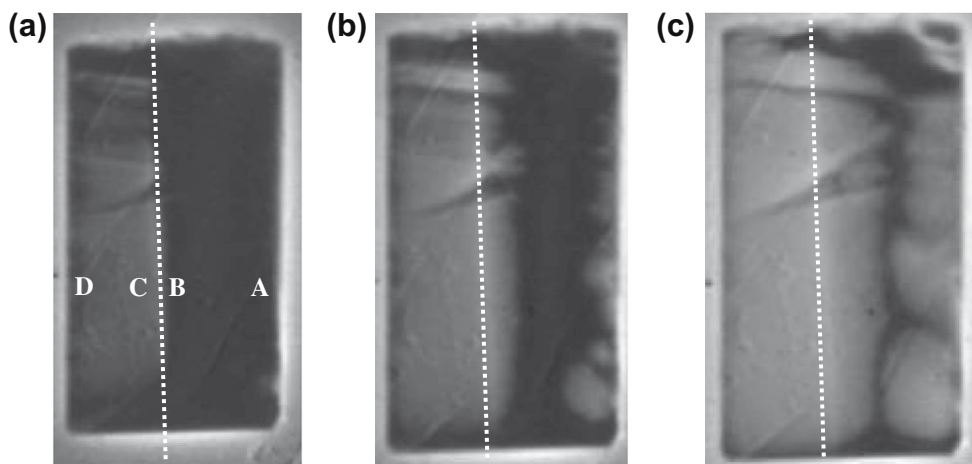


**Fig. 1.** Magneto-optical images of flux penetration through the edges of a partially irradiated  $\text{Bi}_2\text{Sr}_2\text{CaCu}_2\text{O}_{8+\delta}$  sample subjected to external field ramped at 5 Oe/s, 7 (a) 12 (b) and 19 (c) seconds after the application of the field. The dotted line marks the border between the irradiated (right hand side) and pristine parts of the sample. The color tone is brighter for larger inductions. Points A, B, C and D mark locations where magnetization curves in Figs. 2 and 9 were extracted.

One clearly sees that flux penetrating through the sample edges advance in the pristine region (right hand side in each image) at a much higher rate, allowing flux injection from the pristine into the irradiated part through the sharp border between them. Thus, the partially irradiated sample allows simultaneous study and comparison of the metastable vortex state created by flux injection through both the sample edges and the border between the irradiated and pristine parts of the sample.

Fig. 2 exhibits local magnetization curves,  $m = \text{Bloc} - H$  versus the applied field  $H$ , measured at points A and D near the sample edges at 28 K, in the pristine (a) and the irradiated (b) region, respectively (see Fig. 1 for the location of these points). The different curves in each figure correspond to different ramping rate of the external field from 2.5 to 160 Oe/s. Notable differences in the local magnetic response of the pristine and the irradiated parts are evident: In the irradiated part the second magnetization peak is smeared, exhibiting onset at lower fields, and stronger dependence of the onset field on the ramping rate  $dH/dt$  of the applied field. As discussed below, the onset field,  $H_{on}$ , signifies the first field at which MDS is injected into the sample. In the pristine region  $H_{on}$  can be accurately determined; in this region the difference between the persistent current of the ordered state,  $j_{low}$ , and the metastable disordered state,  $j_{high}$ , is large. As a result, the natural increase with field of the local magnetization,  $m$ , is disrupted abruptly by penetration of a metastable disordered vortex state (MDS) through the edges, creating an SMP with a well defined onset. A difficulty in accurate determination of  $H_{on}$  arises in the irradiated region where the difference between  $j_{low}$  and  $j_{high}$  is smaller. As a result, the natural increase of  $m$  is competing with a decrease of  $m$  at a comparable rate, creating a smeared onset. In this case we define  $H_{on}$  as the field where the increase and decrease in  $m$  are exactly compensated, i.e. at the maximum point of  $m$ . We note that this definition of  $H_{on}$  underestimates the shift down of the onset field in the irradiated region.

Fig. 3 shows the onset field,  $H_{on}$ , as a function of  $dH/dt$  in the pristine and irradiated regions. As expected, both curves exhibit accelerated approach of  $H_{on}$  to the thermodynamic order–disorder transition field  $B_{od}$  for  $dH/dt$  approaching zero [28]. However, the curve corresponding to the irradiated region is far below that corresponding to the pristine region, indicating longer lifetime of the MDS in the irradiated part, enabling it to persist at lower fields.

It is important to note that  $H_{on}$  is independent of the measuring location, in both the pristine and the irradiated regions. The reason for it is well understood; as stated above,  $H_{on}$  signifies the first field

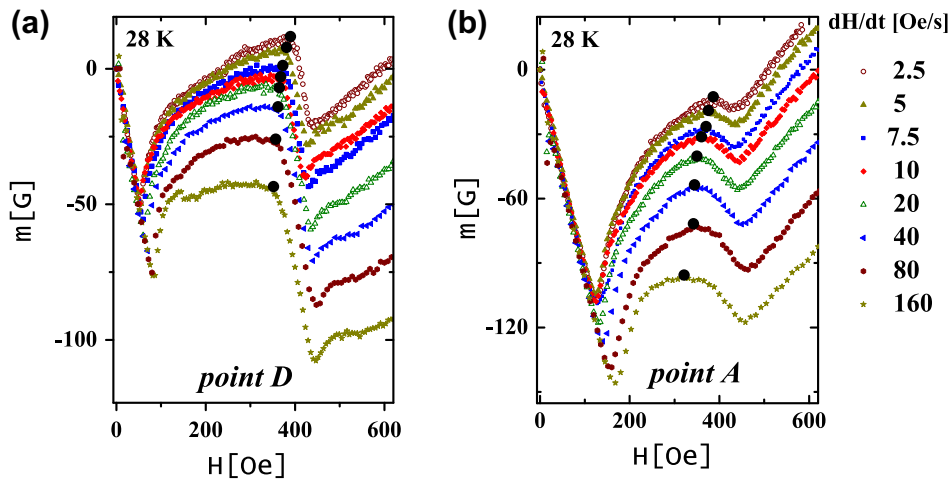


Fig. 2. Local magnetization curves measured in the pristine (a) and the irradiated part (b) of the sample, points D and A, respectively, at 28 K, for various ramping rates of the external field ranging from 2.5 Oe/s to 160 Oe/s.

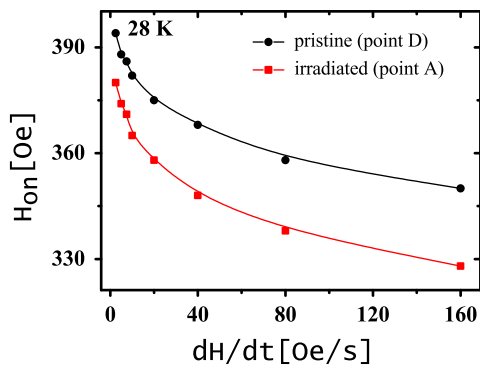


Fig. 3. Onset of the second magnetization peak,  $H_{on}$ , as a function of the rate of change of the external field in the pristine (circles) and irradiated (squares) parts of the sample.

at which MDS is injected into the sample. Appearance of MDS at the sample edge, increases the induction slope near the edge, and thus lowers the induction profile throughout the entire sample, giving rise to a sudden decrease in the local magnetization  $m$  everywhere. As the MDS penetrates deeper into the sample,  $m$

continues to drop until the front of the MDS reaches the location where  $m$  is measured. After the MDS front passes this location,  $m$  is determined solely by the high current density  $j_{high}$  characterizing the disordered state. Further increase of the field causes a decrease of  $j_{high}$  and thus an increase of  $m$ . Experimental verification of the independence of  $H_{on}$  on the measurement location is demonstrated in Fig. 4 which shows local magnetization curves measured at different locations in field ramped at a constant rate of 20 Oe/s. It is clearly observed that the onset field is the same, independent of the location, in both the pristine (Fig. 4a) and irradiated (Fig. 4b) regions. We thus conclude that the curves shown in Fig. 3 characterize the behavior of  $H_{on}$  everywhere in the pristine or the irradiated regions of the sample far away from the border between them.

In the following we argue that the appearance of the MDS at significantly lower fields in the irradiated region signifies both, a slight shift down of the thermodynamic order–disorder transition induction  $B_{od}$ , and a significant increase in the intrinsic lifetime of the MDS. It was previously shown [28] that the first field,  $H_{on}$ , at which the MDS is injected into the sample, is related to the lifetime  $\tau(B)$  of the MDS and the rate of change of the applied field:

$$(\partial\tau/\partial B)_{B=H_{on}} = \frac{1}{dH/dt}. \quad (1)$$

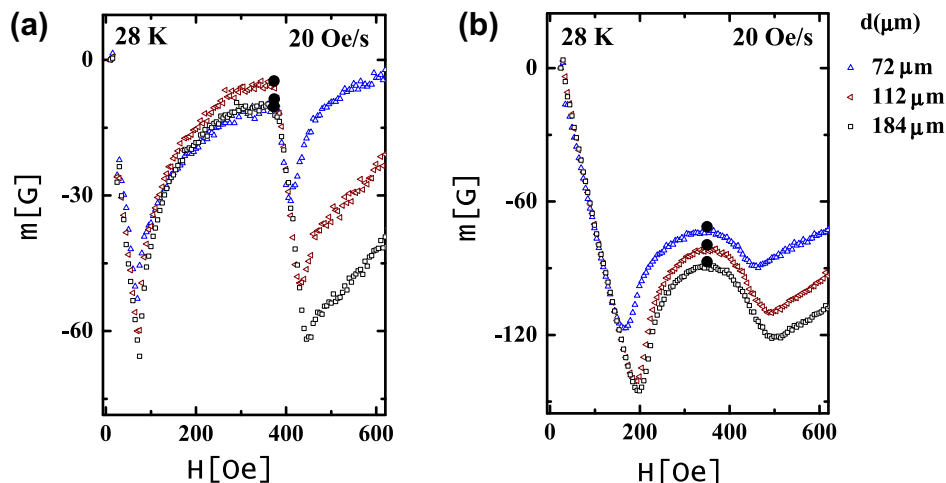


Fig. 4. Magnetization curves at different locations,  $d$ , in the pristine (a) and irradiated (b) regions of the sample. The location  $d$  is measured relative to the respective edge. Note that the onset field of the second magnetization peak is independent of location in both regions.

It was also shown that, at constant temperature, as  $B_{od}$  is approached,  $\tau$  diverges as [28]

$$\tau = \frac{\tau_0}{(1 - B/B_{od})^\gamma}, \quad (2)$$

where  $\tau_0$  is constant and the exponent  $\gamma \approx 2.5$ . Using this value of  $\gamma$ , one obtains the following relationship between  $H_{on}$  and  $dH/dt$ :

$$(B_{od}/2\tau_0)(1 - H_{on}/B_{od})^{7/2} = dH/dt. \quad (3)$$

Thus, a plot of  $(dH/dt)^{2/7}$  versus  $H_{on}$  should yield a straight line that extrapolates to  $B_{od}$  as  $dH/dt$  approaches zero. Such plots, based on the data of Fig. 3, are presented in Fig. 5 for the pristine (circles) and irradiated (squares) regions. The linear fits, presented by the solid lines, show good agreement with the experimental data, thus justifying the empirical Eq. (2) with  $\gamma = 2.5$ . Extrapolations of these linear curves to  $dH/dt = 0$  yield values of 413 and 402 G for  $B_{od}$  in the pristine and irradiated regions of the sample, respectively. Once  $B_{od}$  has been determined,  $\tau_0$  can be calculated from the slopes of the linear curves of Fig. 5. One obtains the values 1.9 and 3.8 ms for  $\tau_0$  for the pristine and irradiated regions, respectively.

An alternative way to quantify the effect of CD on  $B_{od}$  and  $\tau_0$  is by analyzing the lifetime  $\tau(B)$  of the MDS in the pristine and irradiated regions. Knowledge of  $H_{on}$  for different  $dH/dt$  allows determination of  $\partial\tau/\partial B$ , and thus  $\tau(B)$ , using Eq. (1). Results for  $\partial\tau/\partial B$  as a function of  $B$  at 28 K are shown in Fig. 6 for both the pristine (circles) and irradiated regions (squares). Fits to Eq. (2) (solid lines) yield values of 418 and 405 for  $B_{od}$ , and values of 2.2 and 4.1 ms for  $\tau_0$  in the pristine and irradiated regions, respectively, in good agreement with the values obtained in the previous analysis.

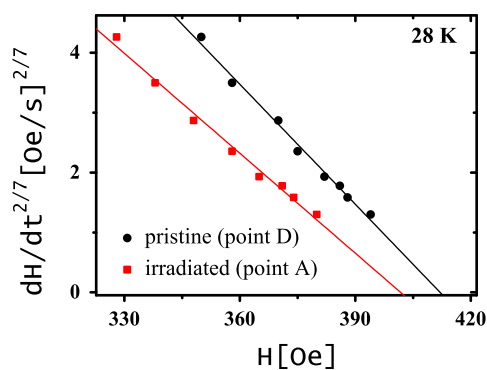


Fig. 5. Plots of  $(dH/dt)^{2/7}$  versus  $H_{on}$  for the pristine (circles) and irradiated (squares) regions of the sample.

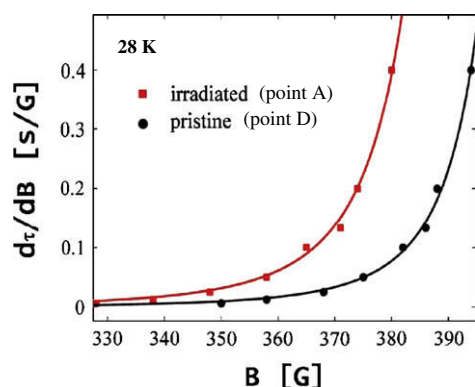


Fig. 6.  $\partial\tau/\partial B$  as a function of  $B$  at 28 K in the pristine (circles) and irradiated (squares) regions. The solid lines are fits to Eq. (2).

Our analysis clearly shows that the CD slightly reduce  $B_{od}$  and significantly increase  $\tau_0$ . Both effects are responsible for the shift of the metastable region to lower fields in the irradiated region. In Fig. 7 we eliminated the effect of lowering  $B_{od}$  by plotting  $\tau$  versus  $B/B_{od}$  using the parameters obtained from the fits of Fig. 6 for points A and D. One clearly sees that in the irradiated region the lifetime of the MDS is intrinsically longer.

Analyses of local magnetic measurements performed at different temperatures yielded similar results. In the irradiated region, the thermodynamic transition induction  $B_{od}$  is slightly lower and the lifetime parameter  $\tau_0$  is longer. As expected, with increasing temperature the columnar defects become less effective and the differences between the pristine and irradiated regions diminish. The solid lines in Fig. 8 are fits to the Arrhenius law  $\tau_0 = t_0 \exp(U/kT)$ . These fits yield values of  $5.5 \times 10^{-5}$  and  $1.7 \times 10^{-5}$  seconds for  $t_0$  and 140 and 187 K for  $U$  in the pristine and irradiated regions, respectively, indicating that in order to relax to the thermodynamic quasi-ordered state vortices in the irradiated region have to overcome a higher energy barrier.

The partially irradiated sample allows studying creation of MDS as a result of injection of ordered vortices through the interface separating the pristine and the irradiated regions of the sample. Such a study is of interest, as it is generally accepted that MDS are created by injection of vortices through inhomogeneous edges [18–20]. Fig. 9a and b shows local magnetization curves measured at two adjacent points across the interface (points C and B in Fig. 1,

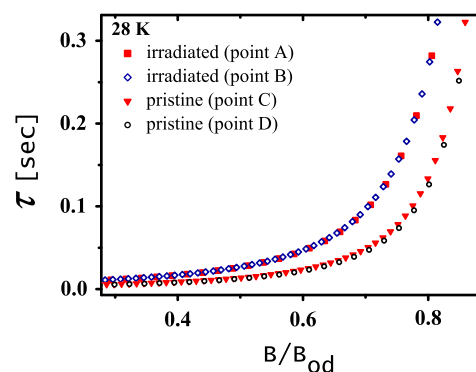


Fig. 7. Life time,  $\tau$ , as a function of normalized induction  $B/B_{od}$  for flux injection through the sample edges (points A, squares and point D, circles) and through the interface between the pristine and irradiated regions (point C, triangles and point B, diamonds).  $B_{od} = 418$  and 405 G, for the pristine and the irradiated regions, respectively.

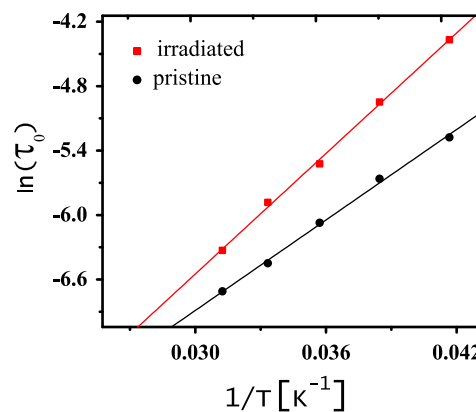


Fig. 8.  $\ln(\tau_0)$  versus inverse temperature in the pristine (circles) and irradiated (squares) regions. Solid lines are fits to Arrhenius law.



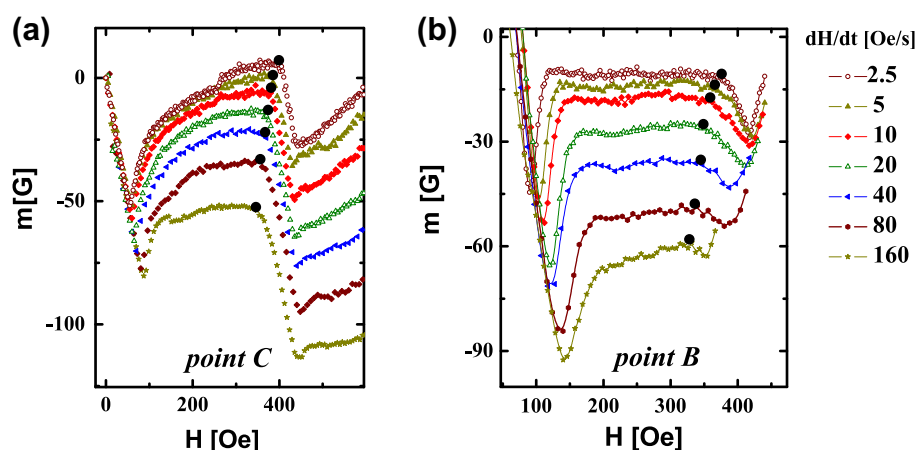


Fig. 9. Local magnetization curves measured at two adjacent points across the interface: point C in the pristine region (a) and point B in the irradiated region (b).

respectively). The onset induction of the second magnetization peak measured at point C, in the pristine side of the border, (Fig. 9a) is consistently higher than that measured at point B in the irradiated side of the border (Fig. 9b). Keeping in mind that the onset in the pristine region signifies the first penetration of MDS into the edge of that part of the sample, the lower  $H_{on}$  values in the irradiated part indicate that quasi-ordered vortices in the pristine region transformed into a disordered state upon crossing the border into the irradiated region. We utilized the dependence of  $H_{on}$  on the ramping rate  $dH/dt$  (Eq. (1)) [32] to calculate the lifetime  $\tau$  of the MDS so generated, following the method described above. The results are added to Fig. 7 (diamonds) together with the results obtained above for flux injection through the sample edges (squares). Evidently, the two sets of data fall on similar curves, indicating that the lifetime of the MDS is an intrinsic property of the sample bulk, independent of the way by which the MDS were created. The ability to create MDS within the bulk of the sample, demonstrated here, challenges the commonly accepted view that edge contaminations are the sole source responsible for the creation of MDS.

#### 4. Summary and conclusions

Our measurements and analyses indicate the unexpected result that dilute CD affect the melting line and the solid–solid phase transition line differently. CD are known to shift the melting line upward [5] while point defects shift it downward [3]. Our results indicate that CD tend to shift the solid–solid line slightly downward rather than upward. While the effect of CD on the solid–solid transition line is minute, their effect on the MDS, created in the vicinity of this line, is considerably larger. We found that the CD significantly increase the lifetime of the MDS, shifting the MDS region to lower fields far from the transition, where in a pristine sample their lifetime is practically zero. Viewing the disordered phase as a state in which vortices are entangled, our results indicate that CD hinder disentanglement of the MDS, contrary to the expectation that CD may stretch the entangled vortices, and in accordance with the observation of Verden in  $\text{NbSe}_2$  [11].

Creating pristine and irradiated regions on the same sample, with a sharp border between them, allowed us to demonstrate the generation of MDS as a result of injection of ordered vortices from the pristine region into the irradiated region through the interface. This result indicates the possibility of a bulk related mechanism which creates MDS in a bulk of a sample with CD. Creation of MDS within the bulk of a sample challenges the commonly accepted view that edge contaminations are the sole source responsible for the creation of MDS.

#### Acknowledgments

This article is dedicated to the memory of Avi Szanto, a devoted colleague and dear friend, whose technical help and unfailing support were crucial in developing this laboratory. We are indebted to C. Trautmann and the Material Research group at GSI Helmholtz Centre for Heavy Ion Research (Darmstadt, Germany), for irradiating the BSCCO crystal. We thank Doron Barnes for helpful discussions and continuous support. This research was supported in part by the Israel Science Foundation, Grant No. 499/07.

#### References

- [1] G. Blatter, M.V. Feigel'man, V.B. Geshkenbein, A.I. Larkin, V.M. Vinokur, *Rev. Mod. Phys.* 66 (1994) 1125; E.H. Brandt, *Rep. Prog. Phys.* 58 (1995) 1465; D.R. Nelson, V.M. Vinokur, *Phys. Rev. B* 48 (1993) 13060 (10A); I. Larkin, V.M. Vinokur, *Phys. Rev. Lett.* 75 (1995) 4666.
- [2] M. Konczykowski, F. Rullier-Albenque, E.R. Yacoby, A. Shaulov, Y. Yeshurun, P. Ljay, *Phys. Rev. B* 44 (1991) 7167; W. Gerhäuser, G. Ries, H.W. Neumüller, W. Schmidt, O. Eibl, Seemann-Ischenko, S. Klaumuzer, *Phys. Rev. Lett.* 68 (1992) 879; L. Klein, E.R. Yacoby, Y. Yeshurun, *Phys. Rev. B* 48 (1993) 3523; M. Konczykowski, V.M. Vinokur, F. Rullier-Albenque, Y. Yeshurun, F. Holtzberg, *Phys. Rev. B* 47 (1993) R5531; L. Klein, E.R. Yacoby, A. Tsamerer, Y. Yeshurun, K. Kishio, *J. Appl. Phys.* 75 (1994) 6322; R.C. Budhani, W.L. Holstein, M. Suenaga, *Phys. Rev. Lett.* 72 (1994) 566; M. Konczykowski, N. Chikumoto, V.M. Vinokur, M.V. Feigelma, *Phys. Rev. B* 51 (1995) 3957; C.J. van der Beek, M. Konczykowski, V.M. Vinokur, T.W. Li, P.H. Kes, G.W. Crabtree, *Phys. Rev. Lett.* 74 (1995) 1214; A. Samoilov, M.V. Feigelma, M. Konczykowski, F. Holtzberg, *Phys. Rev. Lett.* 76 (1996) 2798; W.S. Seow, R.A. Doyle, A.M. Campbell, G. Balakrishnan, D. McK. Paul, K. Kadowaki, G. Wirth, *Phys. Rev. B* 53 (1996) 14611; R.A. Doyle, W.S. Seow, Y. Yan, A.M. Campbell, T. Mochiku, K. Kadowaki, G. Wirth, *Phys. Rev. Lett.* 77 (1996) 1155; L.M. Paulius, J.A. Fendrich, W.-K. Kwok, A.E. Koshelev, V.M. Vinokur, G.W. Crabtree, B.G. Glabola, *Phys. Rev. B* 56 (1997) 913; N. Morozov, M.P. Maley, L.N. Bulaevskii, J. Sarrao, *Phys. Rev. B* 57 (1998) R8146.
- [3] B. Khaykovich, M. Konczykowski, E. Zeldov, R.A. Doyle, M. Majer, P.H. Kes, T.W. Li, *Phys. Rev. B* 56 (1997) R517.
- [4] B. Khaykovich, M. Konczykowski, K. Teitelbaum, E. Zeldov, H. Shtrikman, M. Rappaport, *Phys. Rev. B* 57 (1998) R14088.
- [5] S.S. Banerjee, A. Soibel, Y. Myasoedov, M. Rappaport, E. Zeldov, M. Menghini, Y. Fasano, F. De la Cruz, C.J. van der Beek, M. Konczykowski, T. Tamegai, *Phys. Rev. Lett.* 90 (2003) 087004.
- [6] M. Menghini, Yanina Fasano, F. de la Cruz, S.S. Banerjee, Y. Myasoedov, E. Zeldov, C.J. van der Beek, M. Konczykowski, T. Tamegai, *Phys. Rev. Lett.* 90 (2003) 147001.
- [7] S.S. Banerjee, S. Goldberg, A. Soibel, Y. Myasoedov, M. Rappaport, E. Zeldov, F. de la Cruz, C.J. van der Beek, M. Konczykowski, T. Tamegai, *Phys. Rev. Lett.* 93 (2004) 097002.
- [8] M. Konczykowski, C.J. van der Beek, E. Zeldov, Ming Li, P.H. Kes, *Physica C (Amsterdam)* 408 (2004) 547.

- [9] N. Avraham, Y.Y. Goldschmidt, J.T. Liu, Y. Myasoedov, M. Rappaport, E. Zeldov, C.J. van der Beek, M. Konczykowski, T. Tamegai, Phys. Rev. Lett. 99 (2007) 087001.
- [10] T. Verdene, H. Beidencopf, Y. Myasoedov, H. Shtrikman, M. Rappaport, E. Zeldov, T. Tamegai, Phys. Rev. Lett. 101 (2008) 157003.
- [11] T. Verdene, Study of the dynamic and thermodynamic vortex matter phase diagram in high- $T_c$  and low- $T_c$  type-II superconductors, Ph.D. Thesis, Weizmann Institute of Science, 2008.
- [12] S. Tyagi, Y.Y. Goldschmidt, Phys. Rev. B 67 (2003) 214501.
- [13] C. Dasgupta, Oriol T. Valls, Phys. Rev. Lett. 91 (2003) 127002.
- [14] Y. Nonomura, X. Hu, Europhys. Lett. 65 (2004) 533.
- [15] Y.Y. Goldschmidt, E. Cuansing, Phys. Rev. Lett. 95 (2005) 177004.
- [16] C.J. van der Beek, S. Colson, M.V. Indenbom, M. Konczykowski, Phys. Rev. Lett. 84 (2000) 4196.
- [17] N. Avraham, B. Khaykovich, Y. Myasoedov, M. Rappaport, H. Shtrikman, D.E. Feldman, T. Tamegai, P.H. Kes, M. Li, M. Konczykowski, K. van der Beek, E. Zeldov, Nature (London) 411 (2001) 451.
- [18] Y. Paltiel, E. Zeldov, Y. Myasoedov, M.L. Rappaport, G. Jung, S. Bhattacharya, M.J. Higgins, Z.L. Xiao, E.Y. Andrei, P.L. Gammel, D.J. Bishop, Phys. Rev. Lett. 85 (2000) 3712.
- [19] Y. Paltiel, E. Zeldov, Y.N. Myasoedov, H. Shtrikman, S. Bhattacharya, M.J. Higgins, Z.L. Xiao, E.Y. Andrei, P.L. Gammel, D.J. Bishop, Nature 403 (2000) 398.
- [20] B. Kalisky, Y. Myasoedov, A. Shaulov, T. Tamegai, E. Zeldov, Y. Yeshurun, Phys. Rev. Lett. 98 (2007) 107001.
- [21] D. Giller, A. Shaulov, T. Tamegai, Y. Yeshurun, Phys. Rev. Lett. 84 (2000) 3698.
- [22] H. Kupfer, A. Will, R. Meier-Hirmer, T. Wolf, A.A. Zhukov, Phys. Rev. B 63 (2001) 214521.
- [23] M. Konczykowski, C.J. van der Beek, S. Colson, M.V. Indenbom, P.H. Kes, Y. Paltiel, E. Zeldov, Physica C 341 (2000) 1317.
- [24] D. Giller, B. Kalisky, A. Shaulov, T. Tamegai, Y. Yeshurun, J. Appl. Phys. 89 (2001) 7481.
- [25] D. Giller, A. Shaulov, L. Dorosinskii, T. Tamegai, Y. Yeshurun, Physica C 341 (2000) 987.
- [26] E.Y. Andrei, Z.L. Xiao, W. Henderson, Y. Paltiel, E. Zeldov, M. Higgins, S. Bhattacharya, P. Shuk, M. Greenblatt, Condens. Matter Theories 16 (2001) 241.
- [27] B. Kalisky, D. Giller, A. Shaulov, Y. Yeshurun, Phys. Rev. B 67 (2003) R140508.
- [28] B. Kalisky, Y. Bruckental, A. Shaulov, Y. Yeshurun, Phys. Rev. B 68 (2003) 224515.
- [29] D. Giller, B.Y. Shapiro, I. Shapiro, A. Shaulov, Y. Yeshurun, Phys. Rev. B 63 (2001) R220502.
- [30] N. Motohira, K. Kuwahara, T. Hasegawa, K. Kishio, K. Kitazawa, J. Ceram. Soc. Jpn. 97 (1989) 994.
- [31] J. Wiesner, C. Traeholt, J.-G. Wen, H.-W. Zandbergen, G. Wirth, H. Fuess, Physica C 268 (1996) 161.
- [32] In calculating  $\tau$  in the irradiated part for MDS injected through the interface, one should take  $dB/dt$  were  $B$  is the induction in the pristine regime near the interface. However, experimentally we find  $dB/dt = dH/dt$ .